Desired Order Continuous Polynomial Time Window Functions for Harmonic Analysis

Puneet Singla, *Member, IEEE*, and Tarunraj Singh

***Abstract*—An approach for the construction of a family of desired order continuous polynomial time window functions is presented without self-convolution of the parent window. The higher order of continuity of the time window functions at the boundary of the observation window helps in suppressing the spectral leakage. Closed-form expressions for window functions in the time domain and their corresponding Fourier transform are derived. The efficacy of these new window functions in discerning the weak signal is demonstrated by computer simulations.**

***Index Terms*—Discrete Fourier transforms (DFTs), harmonic analysis, signal analysis, signal detection, spectral leakage.**

I. Introduction

THE FAST Fourier transform (FFT) is widely used to measure the frequency content of sampled measurement data. The FFT analysis is based on a finite sampled data set and assumes circular topologies for both time and frequency domains. In other words, two endpoints of the time waveform are interpreted as though they are connected together. As a consequence of this, the truncated waveform exhibits different spectral characteristics from the original continuous-time signal. Time window functions are used to obtain a continuous waveform without any discontinuities and hence minimize this effect known as *spectral leakage*. Time window functions shape the finite-time sampled measurement data to minimize the edge effects that result in spectral leakage in the FFT spectrum. Time window functions play an important role in digital signal processing, system identification, digital filter design, and other applications.

A detailed analysis and comparison of the different window functions is presented in the seminal work of Harris [1]. Harris introduced a number of figures of merit (FOMs) to evaluate the spectral leakage error, allowing objective comparison between different window functions. Harris, and later Geckinli and Yavuz [2], discussed that spectral leakage can be suppressed by reducing the order of discontinuity at the boundary of observation windows. The discontinuity of the windowed signal can be avoided by matching as many orders of derivatives (of the weighted data) as possible at the boundary, which is equivalent to setting the values of derivatives of the window functions to zero. This is generally achieved by self-convolving a parent window function multiple times in the time domain [1]. For instance, a $\mathcal{C}^m$-continuous time window function can be obtained by applying m time convolution of the $\mathcal{C}^0$-continuous rectangular window. Although the window function generated by m-fold self-convolution of a parent window of length N may exhibit better performance in suppressing spectral leakage than the parent window function, it will also increase the length of the resulting window to approximately mN. Furthermore, the Fourier transform of the resulting window function will have m repeated zeros at each location where the parent window transform had a zero. Ideally, these additional zeros can be better placed between existing zeros to further reduce the sidelobes and better detect weak signals [1].

Furthermore, in [3]–[8], the effects of windowing on the signal-to-noise ratio, harmonic distortions, multifrequency parameter estimation, and quasi-synchronous sampling are studied in detail. It has been concluded that no window function is the best in all aspect, and one should select a window function according to the requirement of a particular application. For example, the Hanning window function is considered useful for noisy measurements, whereas Kaiser–Bessel is recommended to detect two tones with frequencies very close to each other but with very different amplitudes. Over time, many different window functions [9]–[14] have been derived to optimize some features of a window function and for easy implementation. In [9], new window functions have been derived with very good sidelobe behavior, whereas in [10], time window functions are derived from B-splines that have fast sidelobe decay and maximum variance in the time domain. In [11], extremely flattop window functions are derived by multiple time convolution of the weighted cosine windows with parameters optimized for flatness of the main lobe. References [12]–[14] present window functions derived from hyperbolic functions and amplitude-shaping pulses.

In this paper, we present an approach for the construction of a family of polynomial time window functions that allow desired order of continuity at the boundary of observation windows. It is well known that if the mth derivative of a window function is discontinuous, then the sidelobes of window functions asymptotically decay as $6m$ dB/oct [1], [2]. The freedom to choose window continuity at the boundary of the observation window allows us to tradeoff between different merits of the window functions. Another advantage of these window functions is that all their coefficients are integers, and thus, they are easy to evaluate. The structure of this paper is as follows: First, a closed-form expression for a desired order continuous polynomial window function in the time domain is derived, followed by the Fourier transform of these functions.

Manuscript received June 4, 2009; revised October 12, 2009; accepted September 29, 2009. The Associate Editor coordinating the review process for this paper was Dr. Jesús Ureña.

The authors are with the Department of Mechanical and Aerospace Engineering, University at Buffalo, Buffalo, NY 14260 USA (e-mail: psingla@buffalo.edu; tsingh@buffalo.edu).

Color versions of one or more of the figures in this paper are available online at http://ieeexplore.ieee.org.

Digital Object Identifier 10.1109/TIM.2009.2036400

Furthermore, these window functions are compared with conventional window functions on the basis of FOMs, such as equivalent noise bandwidth (ENBW), sidelobe fall off, coherent gain (CG), and scallop loss.

II. Polynomial Time-Domain Window Functions

In this section, we will present an approach for the construction of polynomial window functions in the time domain, which allow desired order of continuity at the boundary of the observation window. Without any loss of generality, we assume the window interval to be $[-1, 1]$. Let us assume that $f(t)$ represents the signal of interest and $\bar{f}(t)$ is the windowed approximation of $f(t)$ over the windowed interval $[-1, 1]$, i.e.,

$$\bar{f}(t) = w(t)f(t) \tag{1}$$

where $w(t)$ is the window function with a compact support over $[-1, 1]$. The requirement that the windowed approximation $\bar{f}(t)$ in (1) forms an mth-order continuous signal leads to the two requirements for the necessary window functions.

1) The first derivative of the window function must have m repeated zeros at the centroid of the windowed interval, i.e., at $t = 0$ with

$$w(0) = 1, \quad \left.\frac{d^k w}{dt^k}\right|_{t=0} = 0, \qquad k = 1, \ldots, m. \tag{2}$$

2) The window function must have an $(m + 1)$th-order zero at the endpoints of the windowed interval, i.e.,

$$w(1) = 0, \quad \left.\frac{d^k w}{dt^k}\right|_{t=1} = 0, \qquad k = 1, \ldots, m. \tag{3}$$

These aforementioned conditions are sufficient to ensure that the value and the first m time derivatives of the windowed signal $\bar{f}(t)$ exactly reduce to the first m time derivatives of the original signal $f(t)$ at the centroid and endpoints of the windowed interval. In our prior work [15], a similar boundary-value problem is solved to generate a special weight function to blend two completely independent adjacent local approximations to a globally valid function. We use the same analysis here to derive a generic expression for an mth-order continuous window function.

Like in [15], we assume that the window function is symmetric around the centroid of the windowed interval $[-1, 1]$, i.e., origin, and develop the expression for the window function valid over the interval [0, 1]. In this respect, we assume the following particular form for the window function:

$$w(t) = 1 - u(t) \tag{4}$$

where $u(t)$ is a polynomial function selected in such a way that the first m time derivatives of the window function vanish at the centroid and endpoints, e.g.,

$$\frac{du(t)}{dt} = Ct^m(1 - t)^m \tag{5}$$

where C is a yet to be defined constant. Now, the remaining boundary conditions, i.e., $w(1) = 0$, can be used to find the constant C as

$$w(1) = 1 - C\int_0^1 \tau^m(1 - \tau)^m d\tau = 0. \tag{6}$$

Now, making use of the fact that the integral expression $\int_0^1 \tau^m(1 - \tau)^m d\tau = (m!)^2/(2m + 1)!$ is a Eulerian integral of the first kind leads to the following value for the constant C:

$$C = \frac{(2m + 1)!}{(m!)^2}. \tag{7}$$

Substituting for the value of C in (5) and substituting the resultant expression in (4) leads to the following expression for the window function:

$$w(t) = w_m(t) = 1 - \frac{(2m + 1)!}{(m!)^2}\int_0^t \tau^m(1 - \tau)^m d\tau. \tag{8}$$

Notice that we use $w_m(t)$ to explicitly indicate the dependence of the window function on the smoothness order m. Furthermore, making use of the binomial theorem to expand the integrand $\int_0^t \tau^m(1 - \tau)^m d\tau$ leads to

$$\begin{aligned} w_m(t) &= 1 - \frac{(2m + 1)!}{(m!)^2}\int_0^t \sum_{n=0}^{m} {}^mC_n \tau^m \tau^{m-n}(-1)^n d\tau \\ &= 1 - K_m \sum_{n=0}^{m} A_{m,n} t^{2m-n+1} \\ {}^mC_n &= \frac{m!}{n!(m - n)!} \end{aligned} \tag{9}$$

where K_m and $A_{m,n}$ are given by the following expressions:

$$K_m = \frac{(2m + 1)!(-1)^m}{(m!)^2} \quad A_{m,n} = \frac{(-1)^n\, {}^mC_n}{2m - n + 1}. \tag{10}$$

Finally, to obtain the expression for the window function in the interval $[-1, 1]$ instead of [0, 1], the absolute value of t can be used as the independent variable rather than t, i.e.,

$$w_m(t) = 1 - K_m \sum_{n=0}^{m} A_{m,n}|t|^{2m-n+1}, \quad -1 \le t \le 1. \tag{11}$$

It should be noted that the exponent of t, i.e., $2m - n + 1$, is always greater than 0. These special functions of (11) are an integral part of the recently developed multiresolution function approximation algorithm known as global–local orthogonal mapping (GLO-MAP) [15], which permit the inclusion of independent local functions over a compact support.

A. Fourier Transformation of Window Functions

In this section, we compute the Fourier transformation of the window functions derived in the previous section.

Let us consider the following Fourier transformation for the window function $w_m(t)$:

$$W_m(\omega) = \int_{-\infty}^{\infty} w_m(t)e^{-i\omega t} dt. \tag{12}$$

Substituting the expression for $w_m(t)$ leads to

$$W_m(\omega) = \int_{-1}^{0} e^{-i\omega t}\left[1 - K_m \sum_{n=0}^{m} A_{m,n}(-t)^{2m-n+1}\right] dt + \int_{0}^{1} e^{-i\omega t}\left[1 - K_m \sum_{n=0}^{m} A_{m,n} t^{2m-n+1}\right] dt. \quad (13)$$

Notice that the first integral expression in (13) is equivalent to

$$\int_{-1}^{0} e^{-i\omega t}\left[1 - K_m \sum_{n=0}^{m} A_{m,n}(-t)^{2m-n+1}\right] dt = -\int_{1}^{0} e^{i\omega t}\left[1 - K_m \sum_{n=0}^{m} A_{m,n} t^{2m-n+1}\right] dt. \quad (14)$$

This leads to

$$\begin{aligned} W_m(\omega) &= \int_{0}^{1} (e^{i\omega t} + e^{-i\omega t})\left[1 - K_m \sum_{n=0}^{m} A_{m,n} t^{2m-n+1}\right] dt \\ &= 2\int_{0}^{1} \cos\omega t \left[1 - K_m \sum_{n=0}^{m} A_{m,n} t^{2m-n+1}\right] dt \\ &= 2\frac{\sin\omega}{\omega} - 2K_{m!}\sum_{n=0}^{m} A_{m,n}\int_{0}^{1} t^{2m-n+1}\cos\omega t dt. \end{aligned} \quad (15)$$

Now let us consider the following integral expression in (15):

$$\begin{aligned} \mathcal{I}_{2m-n+1} &= \int_{0}^{1} t^{2m-n+1}\cos\omega t\, dt = \frac{t^{2m-n+1}\sin\omega t}{\omega}\Big|_0^1 \\ &\quad - \frac{2m-n+1}{\omega}\int_{0}^{1} t^{2m-n}\sin\omega t\, dt \qquad (16) \\ &= \frac{\sin\omega}{\omega} - \frac{2m-n+1}{\omega} \\ &\quad \times\left[-\frac{t^{2m-n}\cos\omega t}{\omega}\Big|_0^1 + \frac{2m-n}{\omega}\int_{0}^{1} t^{2m-n-1}\cos\omega t\, dt\right], \\ &\quad 2m-n>0 \\ &= \frac{\sin\omega}{\omega} + \frac{(2m-n+1)\cos\omega}{\omega^2} \\ &\quad - \frac{(2m-n+1)(2m-n)}{\omega^2}\mathcal{I}_{2m-n-1}, \\ &\quad 2m-n>0. \qquad (17) \end{aligned}$$

Notice that the $2m-n>0$ constraint corresponds to the exponent of t in $\mathcal{I}_{2m-n-1}$ being greater than or equal to zero. Hence, the recursion formula given by (17) is only valid for $2m-n>0$. Consequently, we require $\mathcal{I}_0$ and $\mathcal{I}_1$ to permit us to use the recursion formula given by (17). It is easy to see that $\mathcal{I}_0$ and $\mathcal{I}_1$ are given as

$$\mathcal{I}_0 = \frac{\sin\omega}{\omega} \quad \mathcal{I}_1 = \frac{\cos\omega + \omega\sin\omega - 1}{\omega^2}. \quad (18)$$

Now substituting (17) in (15) leads to

$$\begin{aligned} W_m(\omega) &= \left(2 - 2K_m\sum_{n=0}^{m} A_{m,n}\right)\frac{\sin\omega}{\omega} \\ &\quad - 2K_m\sum_{n=0}^{m} A_{m,n}(2m-n+1) \\ &\quad \times\left[\frac{\cos\omega}{\omega^2} - \frac{(2m-n)}{\omega^2}\mathcal{I}_{2m-n-1}\right], \\ &\quad 2m-n>0. \end{aligned} \quad (19)$$

Making use of the fact that $w(1)=0$ and $dw/dt|_{t=1}=0$ for $m>0$, we get

$$K_m\sum_{n=0}^{m} A_{m,n} = 1 \quad K_m\sum_{n=0}^{m} A_{m,n}(2m-n+1) = 0. \quad (20)$$

Finally, substitution of the identities of (20) in (19) leads to the following generic expression for the Fourier transform of the window function $w_m(t)$:

$$W_m(\omega) = 2K_m\sum_{n=0}^{m}\mathcal{I}_{2m-n-1}A_{m,n}\frac{(2m-n+1)(2m-n)}{\omega^2}, \quad m>0. \quad (21)$$

Table I lists the closed-form expressions for these window functions in the time domain and their corresponding Fourier transforms for different orders of continuity m. Furthermore, the window functions for the first four orders of continuity and their corresponding Fourier transforms are shown in Fig. 1(a) and (b), respectively. From Fig. 1(b), it is clear that the sidelobe far from the main lobe rapidly rolloff with an increase in m. This is consistent with the expected $6(m+1)$ dB/oct rolloff for a window function with an $(m+1)$th-order discontinuous derivative [1], [2]. This attribute is reflected in the reduced spectral leakage. Fig. 1(c) and (d) illustrates the main lobe and a few sidelobes of $W_m(\omega)$, respectively. It is apparent that the width of the main lobe does not significantly change with the order of continuity m. It should be noted that only the curve corresponding to $m=0$ exhibits repeated roots at all locations. This is evidenced by the fact that the slope of $W_m(\omega)$ is zero whenever $W_m(\omega)=0$. This is due to the fact that the window function corresponding to $m=0$ is identical to the Bartlett window, which can be generated by self-convolution of the rectangular window [1]. It is apparent from Fig. 1(d) that increasing the order of smoothness of the window function does not result in repeated roots. This is evidenced by the fact that the slope of $W_m(\omega)$ is discontinuous whenever $W_m(\omega)=0$ for $m>0$.

B. Performance Analysis

To further gain insight into the performance of these window functions, we compute the following FOMs: incoherent power gain (ICG), CG, scalloping loss (SL), and ENBW. ENBW determines the capability of a window function to extract the

TABLE I
WINDOW FUNCTIONS $w_m(t)$ AND THEIR FOURIER TRANSFORM $W_m(\omega)$ FOR DIFFERENT ORDERS OF CONTINUITY m

m	$w_m(t)$	$W_m(\omega)$
0	$1-\lvert t\rvert$	$\frac{2(1-\cos\omega)}{\omega^2}$
1	$1-t^2(3-2\lvert t\rvert)$	$\frac{12(2-2\cos\omega-\omega\sin\omega)}{\omega^4}$
2	$1-\lvert t\rvert^3(10-15\lvert t\rvert+6t^2)$	$\frac{120(12-\omega^2+\omega^2\cos\omega-6\omega\sin\omega-12\cos\omega)}{\omega^6}$
⋮	⋮	⋮
m	$w_m(t)=1-K_m\sum_{n=0}^{m}A_{m,n}\lvert t\rvert^{2m-n+1}$	$2K_m\sum_{n=0}^{m}\mathcal{I}_{2m-n-1}A_{m,n}\frac{(2m-n+1)(2m-n)}{\omega^2}$

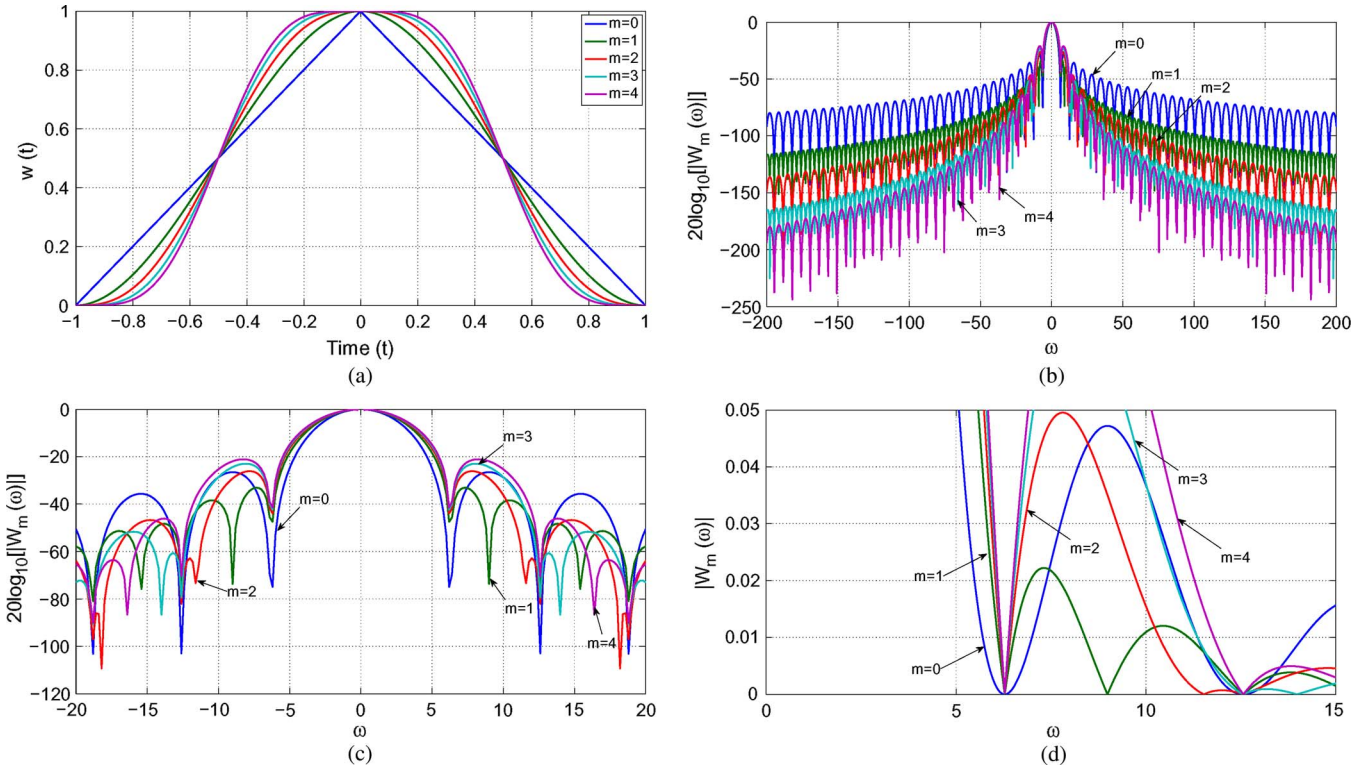

Fig. 1. Window functions $w_m(t)$ and their Fourier transform $W_m(\omega)$ for the first four orders of continuity. (a) $w_m(t)$. (b) 20 $\log_{10}|W_m(\omega)|$ versus ω. (c) Zoom on the main lobe of 20 $\log_{10}|W_m(\omega)|$. (d) Zoom on zeros of $|W_m(\omega)|$.

signal amplitude from background noise and is defined as the width of the discrete Fourier transform (DFT) of a rectangular window with the same peak power gain that would accumulate the same noise power [1]. This can easily be calculated from time samples of the window function $w(nT)$, i.e.,

$$\text{ENBW} = N\frac{\sum_n w^2(nT)}{\left[\sum_n w(nT)\right]^2}. \tag{22}$$

Notice that the lower value for ENBW implies better signal extraction from background noise. The rectangular window has the best possible value for ENBW equal to 1. All other window functions will have ENBW greater than one. Since the window function attenuates the signal at interval ends, it reduces the overall signal power. As a consequence of this, the amplitude measured at the DFT bin is not the same as the real amplitude of the signal's frequency component at that frequency. This reduction in signal power is called the CG and is defined as [1]

$$\text{CG} = \frac{1}{N}\sum_n w(nT). \tag{23}$$

Notice that, for the rectangular window, the CG is 1, whereas for any other window function, the CG is reduced due to the window smoothly going to zero at the boundaries. The ICG represents the accumulated noise power of the window and is computed by making use of the following relationship:

$$\text{ICG} = \frac{1}{N}\sum_n w^2(nT). \tag{24}$$

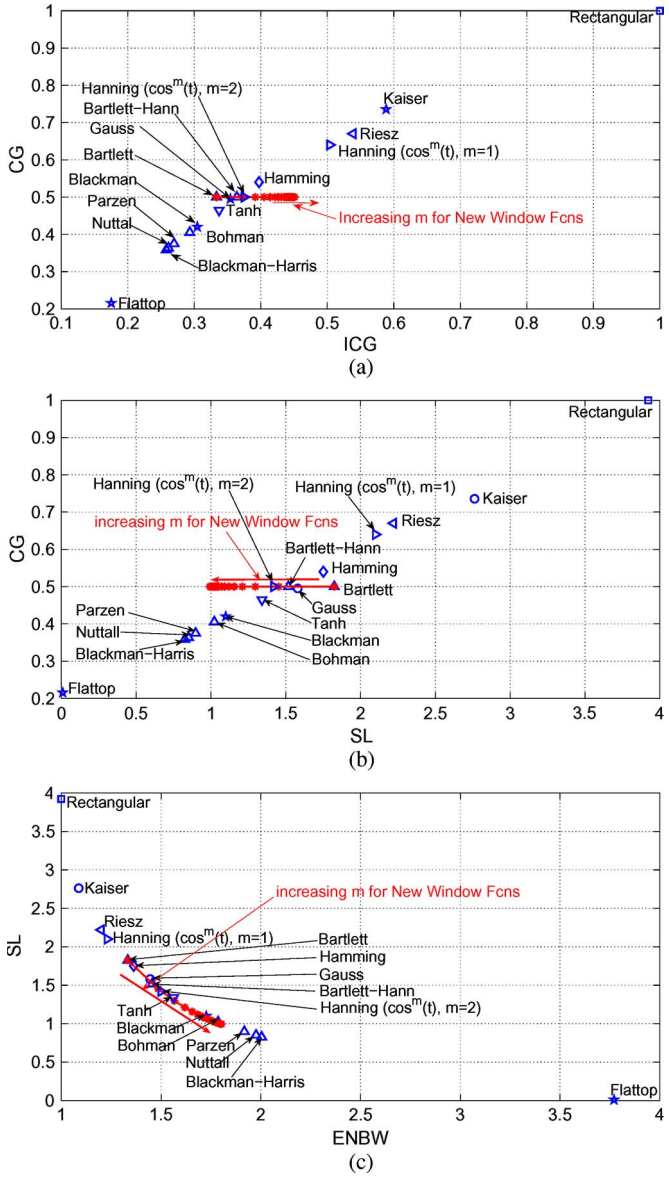

Fig. 2. FOMs for window functions. (a) CG versus ICG. (b) CG versus SL. (c) SL versus ENBW.

Notice that ENBW is equal to the ratio of the ICG to the square of the coherent power gain. Another significant FOM is the SL related to the minimum detectable signal in the worst case of noncoherent sampling. SL is the apparent attenuation of the measured value for a frequency component that falls exactly halfway between DFT bins. It is defined as the ratio of the power gain for a signal frequency component located halfway between DFT bins to the coherent power gain for a signal frequency component located exactly on the DFT bin [1], i.e.,

$$\mathrm{SL} = \frac{\left|\sum_n w(nT)e^{-j\pi\frac{n}{N}}\right|}{\sum_n w(nT)} = \frac{\left|W\left(0.5\frac{\omega_s}{N}\right)\right|}{W(0)}. \qquad (25)$$

Fig. 2(a)–(c) shows the plots of CG versus ICG, CG versus SL, and SL versus ENBW, respectively. As expected, SL decreases while ICG and ENBW increase with an increase in the order of continuity m of the window function. It is interesting to notice that CG remains constant for various orders of continuity. It is also apparent from these plots that the performance of this window function is comparable to many conventional

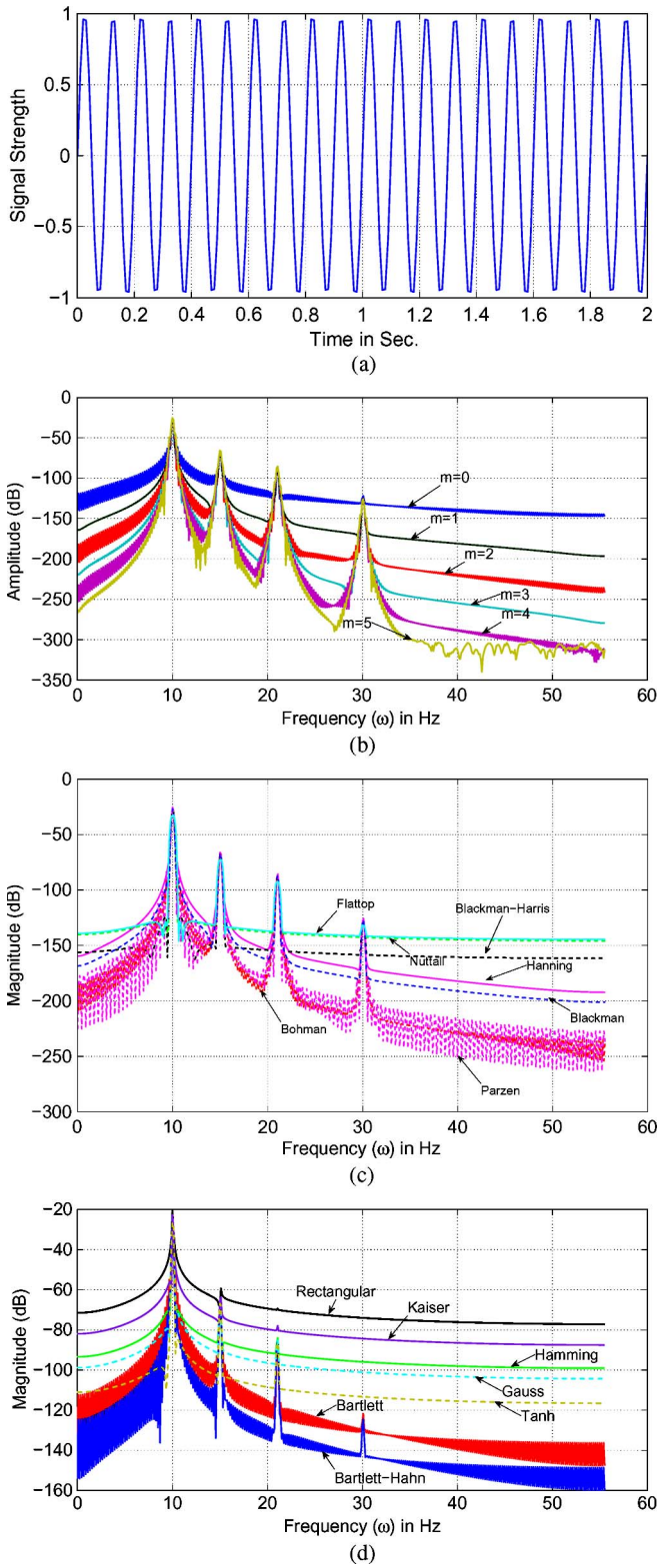

Fig. 3. Example 1: $f(t) = \sin(20\pi t) + 0.01\sin(30\pi t) + 0.001\sin(42\pi t) + 0.00001\sin(60\pi t)$. (a) Signal. (b) DFT of the new windowed signal. (c) DFT of the conventional windowed signal. (d) DFT of the conventional windowed signal.

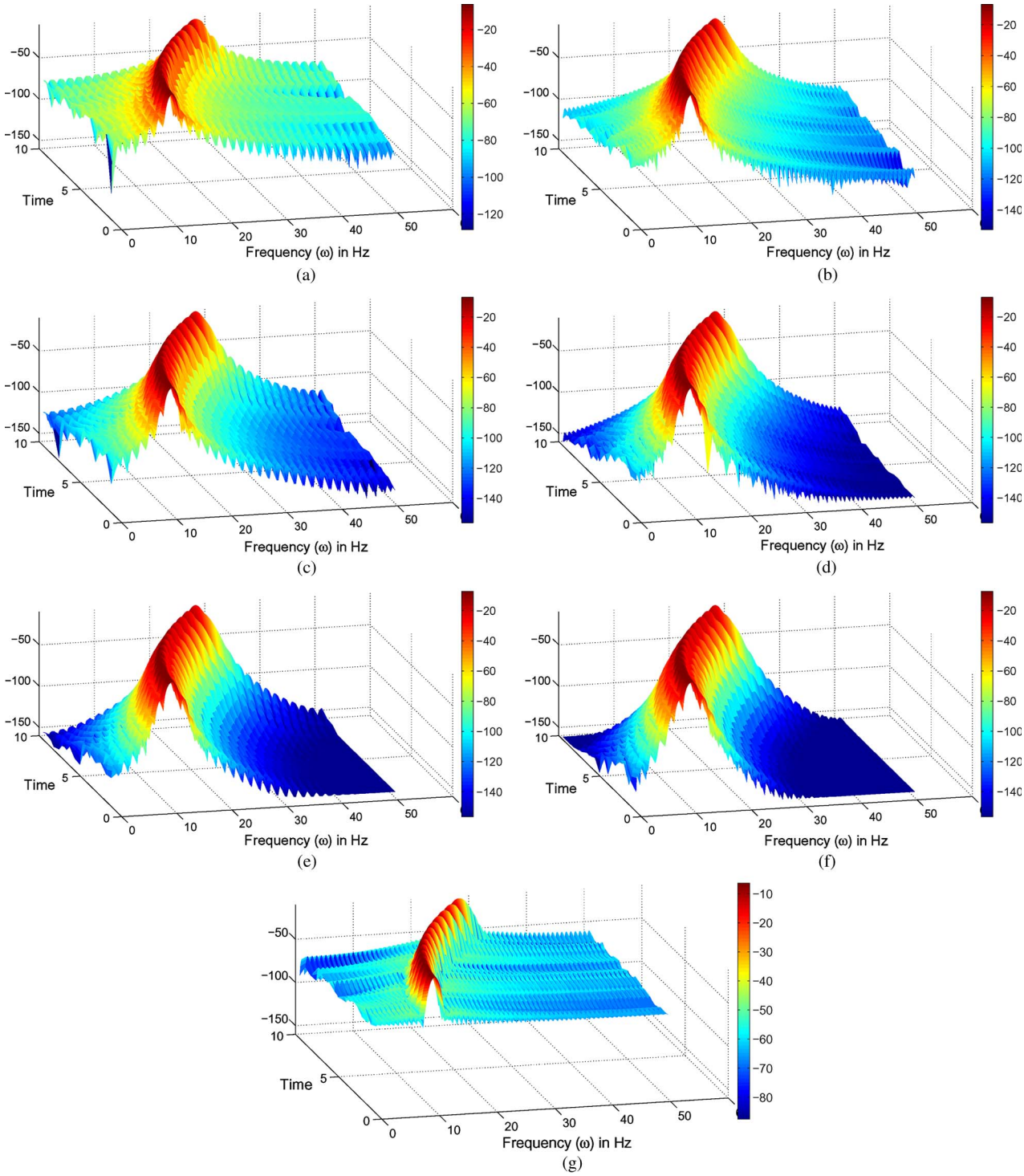

Fig. 4. Example 2: Spectrogram of the chirp signal. (a) $m = 0$. (b) $m = 1$. (c) $m = 2$. (d) $m = 3$. (e) $m = 4$. (f) $m = 5$. (g) Hanning-windowed signal.

window functions, and one can actually tradeoff between different performance criterions by simply changing the order of continuity m.

III. Numerical Results

In this section, two examples are considered to evaluate the performance of the proposed window functions. First, we consider the following benchmark signal $f(t)$ introduced in [12] and [13] to test the efficacy of these new window functions in harmonic signal analysis:

$$f(t) = \sin(20\pi t) + 0.01\,\sin(30\pi t) + 0.001\,\sin(42\pi t) + 0.00001\,\sin(60\pi t). \quad (26)$$

The signal is sampled with $N = 1024$ samples with a sampling frequency of 111 Hz, which is not an integer multiple of frequencies to be identified. Fig. 3(a) shows the plot of a part of the sampled signal. Fig. 3(b) shows the plot of the DFT of the

windowed signal by applying the polynomial window functions corresponding to the first six orders of continuity, whereas Fig. 3(c) and (d) shows the plot of the DFT of the windowed signal by applying conventional window functions available in the MATLAB signal processing toolbox. They have been plotted in separate figures to avoid clutter. From these plots, it is apparent that while many conventional window functions (such as rectangular, Kaiser, Bartlett, Hamming, etc.) struggle in identifying the presence of a weak signal corresponding to a frequency of 30 Hz, the newly developed window functions (except for $m = 0$) correctly identify the relative strength of all frequency tones. This clearly indicates the ability of the new window functions to discern the presence of weak signals. This is anticipated since SL decreases with the increase in the smoothness order m.

The second example corresponds to a chirp signal that generates broadband excitation. The chirp signal is simulated in MATLAB with the frequency swept between 10 and 30 Hz in a quadratic manner. The chirp signal is sampled with $N = 1024$ samples at a sampling frequency of 101 Hz. Fig. 4 illustrates spectrogram plots for new window functions corresponding to $m = 0, \ldots, 5$ and the Hanning window, which is the default window used in the MATLAB *spectrogram* command. As expected, all the plots clearly show the quadratic time variation of the frequency of the signal. It is also clear that as the smoothness index m increases, the spectral leakage rapidly decreases as opposed to the Hanning window. This is a reflection of the rapid sidelobe rolloff of $6(m + 1)$ dB/oct.

IV. Conclusion

Recently developed polynomial blending functions of any desired continuity and with compact support have been exploited as window functions for harmonic analysis. A closed-form expression for the Fourier transform of the proposed polynomial window function has been derived. An advantage of the proposed approach is that it results in desired order continuous window functions without the self-convolution of the parent window function, and thus, the Fourier transform of the resulting window functions does not exhibit repeated zeros at the same location of the $m = 0$ window. The proposed polynomial time window functions are compared with traditional window functions using FOMs, such as CG, ICG power, SL, and ENBW to illustrate their benefits, and their efficacy in discerning the weak signal is illustrated through numerical examples.

Acknowledgment

The authors would like to thank their mentor and friend Prof. J. L. Junkins for introducing them to these amazing window functions.

References

[1] F. Harris, "On the use of windows for harmonic analysis with the discrete Fourier transform," *Proc. IEEE*, vol. 66, no. 1, pp. 51–83, Jan. 1978.

[2] N. Geckinli and D. Yavuz, "Some novel windows and a concise tutorial comparison of window families," *IEEE Trans. Acoust., Speech, Signal Process.*, vol. ASSP-26, no. 6, pp. 501–507, Dec. 1978.

[3] O. M. Solomon, Jr., "The use of DFT windows in signal-to-noise ratio and harmonic distortion computations," *IEEE Trans. Instrum. Meas.*, vol. 43, no. 2, pp. 194–199, Apr. 1994.

[4] C. Offelli and D. Petri, "A frequency-domain procedure for accurate real-time signal parameter measurement," *IEEE Trans. Instrum. Meas.*, vol. 39, no. 2, pp. 363–368, Apr. 1990.

[5] C. Offelli and D. Petri, "Weighting effect on the discrete time Fourier transform of noisy signals," *IEEE Trans. Instrum. Meas.*, vol. 40, no. 6, pp. 972–981, Dec. 1991.

[6] C. Offelli and D. Petri, "The influence of windowing on the accuracy of multifrequency signal parameter estimation," *IEEE Trans. Instrum. Meas.*, vol. 41, no. 2, pp. 256–261, Apr. 1992.

[7] X. Dai and R. Gretsch, "Quasi-synchronous sampling algorithm and its applications," *IEEE Trans. Instrum. Meas.*, vol. 43, no. 2, pp. 204–209, Apr. 1994.

[8] T. Grandke, "Interpolation algorithms for discrete Fourier transforms of weighted signals," *IEEE Trans. Instrum. Meas.*, vol. IM-32, no. 2, pp. 350–355, Jun. 1983.

[9] A. Nuttall, "Some windows with very good sidelobe behavior," *IEEE Trans. Acoust., Speech, Signal Process.*, vol. ASSP-29, no. 1, pp. 84–91, Feb. 1981.

[10] F. Palmieri and L. Bolgiano, Jr., "Window functions obtained from B-S," in *Proc. IEEE ICASSP*, Apr. 1985, vol. 10, pp. 85–88.

[11] I. S. Reljin, B. D. Reljin, and V. D. Papic, "Extremely flat-top windows for harmonic analysis," *IEEE Trans. Instrum. Meas.*, vol. 56, no. 3, pp. 1025–1041, Jun. 2007.

[12] M. Szyper, "New time domain window," *Electron. Lett.*, vol. 31, no. 9, pp. 707–708, Apr. 1995.

[13] S. Saeid and J. Gautam, "New hyperbolic function window family," *Electron. Lett.*, vol. 33, no. 18, pp. 1531–1532, Aug. 1997.

[14] J. de la O Serna, "On the use of amplitude shaping pulses as windows for harmonic analysis," *IEEE Trans. Instrum. Meas.*, vol. 50, no. 6, pp. 1556–1562, Dec. 2001.

[15] P. Singla and J. L. Junkins, *Multi-Resolution Methods for Modeling and Control of Dynamical Systems*. Boca Raton, FL: CRC Press, Aug. 2008.

Puneet Singla (M'99) received the B.S. degree from the Indian Institute of Technology, Kanpur, India, in 2000 and the M.S. and Ph.D. degrees from Texas A&M University, College Station, in 2002 and 2006, respectively, all in aerospace engineering.

He is currently an Assistant Professor of mechanical and aerospace engineering with the University at Buffalo (UB), Buffalo, NY. His work in attitude estimation included algorithms supporting a successful experiment StarNav that won the STS-107. He has authored more than 60 papers to date, including ten journal papers covering a wide array of problems, including attitude estimation, dynamics and control, approximation theory, and uncertainty propagation. He is the principal author of a new textbook entitled *Multi-Resolution Methods for Modeling and Control of Dynamical Systems* (Boca Raton, FL: CRC Press, 2008).

Dr. Singla is a Senior Member of the American Institute of Aeronautics and Astronautics and a member of IEEE and the American Astronautical Society.

Tarunraj Singh received the B.E. degree from Bangalore University, Bangalore, India, the M.E. degree from the Indian Institute of Science, Bangalore, and the Ph.D. degree from the University of Waterloo, Waterloo, ON, Canada, all in mechanical engineering.

He was a Postdoctoral Fellow with the Aerospace Engineering Department, Texas A&M University, College Station. Since 1993, he has been with the University at Buffalo, Buffalo, NY, where he is currently a Professor with the Department of Mechanical and Aerospace Engineering. He was a von Humboldt Fellow and spent his sabbatical at the Technische Universitat Darmstadt, Darmstadt, Germany, and at the IBM Almaden Research Center in 2000–2001. He was a National Aeronautics and Space Administration Summer Faculty Fellow with the Goddard Space Flight Center in 2003. His research has been supported by the National Science Foundation, Air Force Office of Scientific Research, National Security Agency, Office of Naval Research, and various industries, including MOOG Inc. Praxair and Delphi Thermal Systems. He has published more than 150 refereed journal and conference papers and has presented over 35 invited seminars at various universities and research laboratories. His research interests are in robust vibration control, optimal control, nonlinear estimation, and intelligent transportation.